

UCLA

UCLA Previously Published Works

Title

Time-Dependent Measurement of Nrf2-Regulated Antioxidant Response to Ionizing Radiation
Toward Identifying Potential Protein Biomarkers for Acute Radiation Injury

Permalink

<https://escholarship.org/uc/item/Or44v85k>

Journal

Proteomics Clinical Applications, 13(6)

ISSN

1862-8346

Authors

Liu, Kate

Singer, Elizabeth

Cohn, Whitaker

et al.

Publication Date

2019-11-01

DOI

10.1002/prca.201900035

Peer reviewed



Published in final edited form as:

Proteomics Clin Appl. 2019 November ; 13(6): e1900035. doi:10.1002/prca.201900035.

Time-Dependent Measurement of Nrf2-Regulated Antioxidant Response to Ionizing Radiation towards Identifying Potential Protein Biomarkers for Acute Radiation Injury

Kate Liu¹, Elizabeth Singer², Whitaker Cohn², Ewa D. Micewicz², William H. McBride³, Julian P. Whitelegge², Joseph A. Loo^{1,4}

¹Department of Chemistry and Biochemistry, UCLA

²Pasarow Mass Spectrometry Laboratory, Jane and Terry Semel Institute for Neuroscience and Human Behavior, David Geffen School of Medicine, UCLA

³Department of Radiation Oncology, David Geffen School of Medicine, UCLA

⁴Department of Biological Chemistry, David Geffen School of Medicine, Molecular Biology Institute, and UCLA/DOE Institute for Genomics and Proteomics, UCLA

Abstract

Purpose—Potential acute exposure to ionizing radiation in nuclear or radiological accidents presents complex mass casualty scenarios that demand prompt triage and treatment decisions. Due to delayed symptoms and varied response of radiation victims, there is an urgent need to develop robust biomarkers to assess the extent of injuries in individuals.

Experimental design—The transcription factor Nrf2 is the master of redox homeostasis and there was transcriptional evidence of Nrf2-dependent antioxidant response activation upon radiation. We investigated the biomarker potential of Nrf2-dependent downstream target enzymes by measuring their response in bone marrow extracted from C57Bl/6 and C3H mice of both genders for up to 4 days following 6 Gy total body irradiation using targeted mass spectrometry.

Results—Overall, C57Bl/6 mice have a stronger proteomic response than C3H mice. In both strains, male mice have more occurrences of upregulation in antioxidant enzymes than female mice. For C57Bl/6 male mice, 3 proteins showed elevated abundances after radiation exposure:

Correspondence: Julian P. Whitelegge, Pasarow Mass Spectrometry Laboratory, Jane and Terry Semel Institute for Neuroscience and Human Behavior, University of California, Los Angeles, CA 90095, USA jpw@chem.ucla.edu Fax: +1-310-206-2161, Joseph A. Loo, Department of Chemistry and Biochemistry, University of California, Los Angeles, CA 90095, USA, jloo@chem.ucla.edu Fax: +1-310-206-4038.

Associated Data

Raw data and Skyline data repository access:

Thermo raw files have been deposited to PeptideAtlas with the dataset identifier: PASS01319 (<http://www.peptideatlas.org/PASS/PASS01319>)

Username: kateliu@ucla.edu

Password: VW9657n

Skyline files have been deposited to Panorama and can be accessed from

<https://panoramaweb.org/pLJaWf.url>

Email: panorama+loo@proteinms.net

Password: Kh6SM#kn

The authors have declared no conflict of interest.

catalase, superoxide dismutase 1, and heme oxygenase 1. Across both strains and genders, glutathione S-transferase Mu 1 was consistently decreased.

Conclusions and clinical relevance—This study provides the basis for future development of organ-specific protein biomarkers used in diagnostic blood test for radiation injury.

Keywords

Antioxidant response; Bone marrow; Gender difference; Ionizing radiation; Targeted proteomics

1. Introduction

Despite continual risk of radiation from nuclear accidents and terrorist attacks, effective assessment of acute radiation exposure remains to be established for triage and treatment of the population.^[1,2] Following a radiological event, several stages of mass screening utilizing a combination of physical and biological dosimetry methods will be needed to establish the severity of any radiation exposure. Traditionally, clinical determination of radiation dose relies on cytogenetic assays such as chromosome aberration, which normally involves lymphocyte cell culture and scoring of abnormalities. This process is time consuming and requires experienced personnel, making it unsuitable for triage of a mass-casualty event.^[1–3] In addition, cytogenetic assays from blood yields a crude total body dose estimate, which is not ideal given that accidental exposure is likely heterogeneous and there is considerable difference in organ sensitivities to radiation. On the other hand, protein biomarkers can offer molecular insights into the physiology of cells and tissues that can guide organ-specific medical treatment. Despite the advantages of proteomics, it has been underutilized in radiation research historically, which leads to a scarcity in radiation proteomics knowledge^[4] and a shortage of well-established tissue-specific biomarkers.^[5]

Some of the special challenges for proteomic analysis of radiation biology are due to subtle alterations in cell or tissue proteome, even after high dose exposure.^[6] This impacts the majority of radiation proteomics studies and as a result there has been suggestions to apply a fold change cutoff lower than 1.5 for biological significance in radiation research.^[6] In recent years, applications of proteomics in radiation research have increased with advancement in high throughput mass spectrometry technologies. Several groups have developed or implemented state-of-the-art quantitative proteomics tools to identify and validate protein biomarker signatures associated with radiation exposure.^[7–11] Our focus has been on the master regulator of anti-oxidant responses, NF-E2-Related Factor 2 (Nrf2).

Ionizing radiation (IR) causes a multitude of effects on cells. Radiation can directly damage DNA and other biomolecules or indirectly through generation of free radicals and reactive oxygen species (ROS) leading to acute radiation syndromes (ARS) and chronic effects of radiation including carcinogenesis, fibrosis, inflammation, and genomic instability.^[12,13] In an attempt to maintain redox homeostasis, cellular antioxidant defense mechanisms that are composed of small molecular antioxidants and antioxidant enzymes are activated. Many antioxidant enzymes are regulated by a key transcription factor, Nrf2. Nrf2 is normally sequestered by Keap1 protein in the cytoplasm. Upon activation by signals such as ROS, the Nrf2-Keap1 complex is disrupted, leading to nuclear translocation of Nrf2 and binding to the

Antioxidant Response Element (ARE), which in turn regulates expression of downstream antioxidant and detoxification genes that boost cell survival.^[14] These target genes include glutathione S-transferase (GST), UDP-glucuronosyltransferases, γ -glutamylcysteine synthetase (γ -GCS), glutathione peroxidase, superoxide dismutase 1 (SOD1), heme oxygenase 1 (HO-1), catalase, and NADPH: quinone oxidoreductase (NQO-1). These enzymes have been repeatedly demonstrated to be cytoprotective against insult, and Nrf2 is assumed to be a key regulator for inducible expression of these enzymes.^[15,16]

Two articles published in 2010 reported Nrf2 transcriptional activation following ionizing radiation. Tsukimoto *et al.* showed that low dose gamma rays induced Nrf2 activation in mouse macrophage RAW264.7 cells.^[17] A separate study by McDonald *et al.* also observed similar Nrf2 induction in different systems.^[18] They found that single doses of ionizing radiation from 2 to 8 Gy activated ARE-dependent transcription in breast cancer cells in a dose-dependent manner. They also observed increased radiosensitivity in Nrf2 knock out cells and mice after irradiation.^[18] More interestingly, a recent transcriptional study by Purbey *et al.* identified ROS activation of Nrf2 as an important IR sensing pathway.^[19] Their study reveals that Nrf2 activation by ROS is highly selective to radiation exposure as opposed to other environmental insults. In their RNA-Seq data from C57Bl/6 bone marrow derived macrophage (BMDM) collected 0.5–24 hr after 6 Gy irradiation, only 99 genes (1.1%) were induced more than 4-fold, which is in accordance with the common observation of subtle changes in the proteome upon irradiation. Among these few potentially induced genes, Nrf2-regulated gene expression peaked between 1–2 hr and were classified as early response genes.

Besides potent induction of Nrf2 after IR, studies also indicated different induction kinetics in different cell types.^[20] For example, in the two initial reports, Tsukimoto *et al.* observed a rapid induction in mouse RAW264.7 macrophage cells, whereas McDonald *et al.* found a delayed response of 5 days in other cell types. The different induction kinetics can be useful to differentiate the origin of damage. Another factor that can be utilized to localize Nrf2 response is isoform-specific tissue distributions. For instance, GST enzyme is highly polymorphic and it consists of 25 isoforms in mice and also in human (taken from Uniprot). A study mapping out GST tissue distributions in mouse reported differential expression of these isoforms in different tissues, and some isoforms were predominantly expressed in certain tissues.^[21]

Therefore, based on the existing evidence of robust and dose-dependent induction of Nrf2 following IR and other desirable features such as differential induction kinetics and tissue-specific expression, we hypothesized a biomarker potential for Nrf2-mediated response proteins in assessment of ionizing radiation exposure and related organ damage. Potentially, these proteins can be used towards development of a diagnostic blood test for exposure and feedback of efficacy of mitigatory treatment in radiation emergencies.

In this study, using a targeted proteomics approach with mass spectrometry (MS), we examined the response of Nrf2-ARE-dependent enzymes in mouse bone marrow collected at various time points (8 hours to 4 days) after 6 Gy total body irradiation (TBI) in two mouse strains and both genders. The strain and gender groups offer a representation of varied

radiation response in a population due to different genetic backgrounds. Bone marrow is investigated in this initial study because it is a highly radiosensitive organ and the responses of the hematopoietic system are major determinants of outcome after IR exposure.^[22] A high sublethal dose of 6 Gy TBI causes significant damage to bone marrow and hematopoietic acute radiation syndrome (H-ARS) in mice. Nrf2-mediated response is particularly important in this context because Nrf2 activation is also known to enhance hematopoietic stem progenitor cell function and mitigate IR-induced bone marrow suppression and mortality.^[23,24] The measurement of Nrf2-ARE-dependent proteins in bone marrow in this study may provide insights to hematopoietic recovery of mice and this study serves as a foundation to potential subsequent investigations of these signatures in blood. Direct biomarker discovery in blood plasma or serum has not led to many successes in the past because of low abundant disease-related proteins in blood. Instead, approaches such as using proximal fluid and peripheral tissues can be favorable for initial selection of candidates.^[25]

2. Materials and methods

Animals

C3Hf/Sed//Kam and C57Bl/6/JAX gnotobiotic male and female mice were bred and housed in the Radiation Oncology AAALAC-accredited animal facility at UCLA, and utilized at a body weight of 28gms (with 1S.D.<1gm; 9–12wks of age). Mice of both sexes in groups of eight were matched to minimize variation in strain, age, weight and gender. Animal health was monitored at least daily and irradiated mice were followed more closely. Body weight was assessed twice per week. Euthanasia was by exposure to isoflurane and confirmed by cervical dislocation. There were no deaths due to irradiation or experimental procedures as the dose and times were chosen to avoid hematologic ARS. The experiments were approved by the UCLA-IACUC and adhered to all federal and local regulations for the humane treatment of animals.

Irradiation

Total body irradiation was performed using an AEC Gamma Cell 40 cesium irradiator (Cs-137) within the Animal Facility at a dose rate of around 60 cGy/min on unanesthetized mice in a well-ventilated Lucite box. Dosimetry was performed by the CMCR Physics Core at UCLA and involved the use of ionization chambers and chromographic film to assess beam flatness across the field (<5%). The LD70/30 dose for our C3H/Sed mice is 7.73 Gy. For C57Bl/6 mice, it is 8.51 Gy.

Bone Marrow Extraction

At 8 hour, 1, 2 and 4 days after TBI, bone marrow was extracted. The bone marrow was flushed from intact thigh bones of mice and cleaned with 70% ethanol using 5ml 1X PBS. The resulting bone marrow suspension was centrifuged at 1,000 rpm in a clinical centrifuge and the pellet was frozen in a dry ice/ethanol bath and stored at –80°C.

Proteomic Sample Preparation

Bone marrow tissue was lysed in 0.5% (w/v) sodium deoxycholate, 12 mM N-lauroylsarcosine, and 50 mM triethylammonium bicarbonate (TEAB). The samples were homogenized with a bead beater (Bullet Blender; Next Advance, Inc.) at max. speed for 1 min, followed by heating at 95°C for 5 minutes, and sonication in a water bath for 5 min. Samples were centrifuged at 16,000 g for 5 min and supernatants were collected. Protein concentration in the supernatant was measured using a Pierce BCA Protein Assay Kit following the manufacturer's protocols (Thermo Fisher). An aliquot of 50 µg total protein from each sample was reduced with 5 mM tris(2-carboxyethyl)phosphine for 30 min at room temperature and alkylated with 10 mM iodoacetamide in the dark for 30 min at room temperature. The protein samples were then diluted 5 fold with 50 mM TEAB. Trypsin (MS grade; Thermo Pierce) was added at 1/100 enzyme to protein ratio and the sample was incubated at 37°C for 3–4 hours, followed by another 0.5 µg of trypsin addition and overnight incubation at 37°C. Digestion was quenched by 0.5% trifluoroacetic acid. Samples were centrifuged at 16,000 g for 5 min and supernatants were collected and dried under vacuum. Samples were desalted with C18 Stagetips made from Empore C18 solid phase extraction disks. The desalted samples were stored at –80°C until use.

Surrogate Peptide Selection

Proteotypic peptides for Nrf2-modulated proteins were selected from PeptideAtlas (www.peptideatlas.org) with preference for high empirical suitability score, number of observations and proteotypic score. Peptides were filtered according to the following criteria: 8–25 amino acid in length, no missed cleavage site, and no possible modification sites such as cysteine, methionine, tryptophan, and N-terminal glutamine. Candidate peptides were further evaluated by their performance in Parallel Reaction Monitoring (PRM) experiments using a control bone marrow sample. The top 2 peptides were selected as surrogates for each protein for the PRM assay (Table 1). Peptide uniqueness was confirmed by searching against the NCBI Protein Reference Sequence database for *Mus musculus* using BLASTp (exceptions: peptide ITQSNAILR belongs to multiple isoforms of GST proteins and peptide YTGTRPSNLAK belongs to multiple isoforms of UGT).

Crude stable isotope-labeled standard (SIS) peptides (¹³C, ¹⁵N on C-terminal R/K) for the 18 peptides in Table 1 were synthesized by Thermo Pierce. The heavy peptides were diluted with injection buffer (3% acetonitrile, 0.1% formic acid) and pooled to make a final concentration of either 10 nM or 100 nM in the SIS mixture to match the concentrations of endogenous peptides in the sample.

Liquid Chromatography-Mass Spectrometry

Each sample was resuspended in 100 µl injection buffer. An equal volume of SIS mixture was added to the sample for relative quantitation. All samples were subjected to analysis on an Easy-nLC 1000 system coupled to a Q-Exactive mass spectrometer (Thermo Fisher Scientific). The samples were grouped into injection blocks that covered all conditions of comparison (time points, strains, genders). Each block containing 20 samples was injected in a randomized order and analyzed in targeted-MS² mode with retention time scheduling (4 min window). Triplicate injections of 8 biological replicates were analyzed over 480 runs.

An *E.coli* digest standard (1 µg/µl) was analyzed at the start and end of each block to ensure stability of the LC-MS/MS system.

A 4-µl injection was loaded onto a 75 µm i.d. × 25 cm EASY-Spray analytical column (Thermo Fisher Scientific). Peptides were eluted in a 50 min gradient of mobile phase A (0.1% formic acid in water) and mobile phase B (0.1% formic acid in acetonitrile) at a flowrate of 300 nl/min: 5% B at 0 min, 29% B at 32 min, and 80% B from 40.5–50 min. The spray voltage was 2 kV and the capillary temperature was 250 °C. The mass spectrometer was operated in a targeted-MS2 acquisition mode with a maximum IT of 130 ms, 1 microscan, 35 000 resolution, 2E5 AGC target, 1.6 m/z isolation window, and 27% normalized collision energy.

PRM Assay Quantitative Performance

While 18 peptides were monitored in the assay, the 6 most reliable peptides representing 6 proteins were used for final quantitation and these peptides were indicated in Table 1. Linearity of PRM response for these peptides was evaluated by spiking varying amounts of heavy standard peptides into a constant matrix made from pooling C57Bl/6 male control mouse bone marrow digest samples, based on the “reverse curve” method described in Percy, *et al.*[26–29]. The final heavy peptide concentrations in the pool were either 0.05, 0.5, 5, 50, 500 nM or 0.5, 5, 50, 500, 5000 nM depending on the peptide (the range was adjusted to match concentrations of endogenous peptides). Triplicate injections were performed to construct the reverse response curve. The linear range spanned more than four orders of magnitude, and our measurements lay within the linear range of the assay (Supplementary Figure S1).

The extent of carryover was also tested by running replicate injections of 4 randomly chosen samples in different injection orders and compared the peak area ratios of target peptides. No significant differences in the peak area ratios between replicates were observed, suggesting sample carryover in our LC-MS system was minimal. There was also no detectable target peptide in blank runs following sample runs in PRM mode.

Stable Isotope Label-based Relative Quantification

Raw PRM data were processed in Skyline (version 3.6.0, MacCoss lab, University of Washington). Public MS/MS spectral libraries for *Mus musculus* were uploaded to Skyline from National Institute of Standards and Technology and Global Proteome Machine databases. The Uniprot FASTA file for *Mus musculus* (82124 protein entries) was added to Skyline as the background proteome. Extracted chromatograms for target peptides were manually inspected to ensure correct peak detection. Better performing peptides with the top three to five transitions were selected for quantification based on the higher dot product correlation between the observed transitions of target peptides and library spectrum, indicating higher confidence in peptide detection. Summed peak area ratios of endogenous versus SIS peptide transitions were obtained for the preliminary relative quantification result.

Statistical Analysis using MSstats

Statistical analysis was performed with the MSstats package (version 3.6.0) implemented in R. Data were divided into 4 groups: C57 male, C57 female, C3H male, C3H female. Within MSstats, peak intensities were first log₂ transformed, and normalized to equalize medians in log₂ intensities in all runs within a group of comparison. The intensities of the features of a protein in a run were summarized to obtain a single value per protein per run, using Tukey's median polish (accounted for missing values). Finally, to test protein abundances for significant changes of each time point compared to unirradiated control, a linear mixed effect model was applied and adjusted p-values (accounting for multiple comparisons) were obtained.

3. Results and discussion

3.1 PRM assay development and relative quantification result in Skyline

Statistical design of mass spectrometry experiments was taken into consideration in our assay development.^[30] Samples were grouped into randomized injection blocks to minimize instrument bias and batch-to-batch variation over month-long data acquisition. Within each block, there were 20 samples covering all conditions of comparison, including 4 mouse groups (two strains and genders) and 5 time points. Samples were analyzed in random order within each block. Eight blocks of biological replicates were cycled three times to obtain triplicate measurements.

With respect to peptide performance in the PRM assay, six out of the nine putative protein targets were reliably detected in the biological samples. The remaining three proteins had run-to-run inconsistencies either in standard or endogenous peptide levels. The Glutathione Peroxidase 1 standard peptides had too much variation in intensity between different sample preparations, possibly caused by hydrophobicity issues that resulted in variable peptide loss. NAD(P)H dehydrogenase [quinone] 1 and UDP-glucuronosyltransferase 1-1 endogenous peptides were not reliably detected, possibly due to low abundance in this complex matrix. It is conceivable that other more detectable peptides exist for these proteins if we relax the peptide selection criteria, but in doing quantification accuracy may be compromised. For the final analysis, only one best-performing peptide per target protein was included and their top 3-5 transitions based on dot product and reproducibility were used in quantitation. Summed peak area ratios of endogenous versus SIS peptide transitions in Skyline were obtained for visualization of the raw relative quantification result (Figure 1).

3.2 Statistical significant changes using MSstats

Skyline data were imported to MSstats in R to test the statistical significance of protein abundance changes at each time point relative to the unirradiated controls. Data were processed within individual mouse groups. MSstats first log₂-transforms and normalizes intensities in all runs by equalizing the median intensities of the heavy standard peptides. It then generates protein-level summaries for data visualization and quality control after imputation for missing values and removal of poor quality features. Among the visualization outputs generated in this step, a condition plot displays potential systematic differences in protein intensities between conditions (examples shown in Figure 2). Next, to find

differentially abundant proteins, it applies intensity-based linear mixed effect models to determine estimate of protein abundance and variation.^[31] The heatmaps generated from this step provide convenient visualization for strain and gender comparisons (Figure 3).

3.3 Time dependent radiation response in bone marrow

In general, the time course patterns for these proteins are surprisingly complex and reveal progressive changes in the response to radiation in the bone marrow. Specifically, the more frequently studied C57Bl/6 male mice showed elevation of CAT and HMOX1, a decrease in GSTM1 abundance, a biphasic pattern for SOD1, and no prominent change in two GCL subunits (Figure 2). With the expectation that higher antioxidant capacity is needed for cell survival after irradiation, it is surprising to see progressively decreased abundance of GST and GCL enzymes with time given their roles in glutathione homeostasis (Figure 4), which could be due to their overutilization. In contrast, SOD1 and CAT showed a biphasic response that differed in timing between the 2 mouse strains. For these, a nadir was seen at either 8 or 24 hr for most mouse groups (Figure 1), which is in keeping with the findings of the Romeo group.^[32] This biphasic theme that emerged may reflect early and late radiation responses controlled by different mechanisms.^[20] Cellular responses to radiation are multifaceted and persisting. After an initial oxidative insult, a broad range of basal and inducible antioxidant responses is initiated as a cytoprotective shield. Following these early events, cells also undergo further waves of secondary ROS generation, DNA damage, and signaling. These further pro-oxidant responses can persist through multiple cell divisions and manifest differently in different subcellular context. Changes of these Nrf2 target enzymes in our time course data could potentially represent waves of different signals in the cells and their attempts to respond.

Another layer of complexity comes from different radiation sensitivities in different cell types. A high sublethal dose of 6 Gy causes a rapid depletion of cells in the bone marrow and peripheral blood.^[33] In bone marrow, highly proliferative hematopoietic progenitor cells are particularly sensitive and plunge after 6 Gy irradiation, whereas other hematopoietic and mesenchymal cells are more resilient. There is also mass immigration from bone marrow into the circulation, which profoundly alters its composition. This is evident in the color of tissues that ranged from red marrow in control mice to yellow marrow in irradiated mice. These changes and subsequent repopulation can potentially result in disproportionate shifts in protein levels and be impacted by different basal levels of these antioxidant enzymes in various cell types.

3.4 IR-induced alterations in Nrf2-ARE regulated protein targets

Glutamate-Cysteine Ligase—(GCL) enzyme is a heterodimer composed of a modifier (GCLM) and a catalytic (GCLC) subunit that catalyzes the first and rate-limiting step in glutathione (GSH) synthesis (Figure 4). The rate of GSH synthesis is influenced by (1) amount and relative ratios of the two GCL subunits, (2) availability of its substrate, L-cysteine, and (3) extent of feedback inhibition of GCL by GSH.^[34] GCL is predominantly regulated by the Nrf2-ARE pathway at the transcriptional level.^[34,35] Nrf2 knockout mice showed decreased levels of GCLC and GCLM expression.^[35] In our data, we observed progressive decreases in abundance of GCLM in C57 F and C3H M&F mice following 6 Gy

irradiation, but no significant change in GCLC levels (Figure 3). In most tissues, GCLM is thought to be the more rate limiting component and to enhance the catalytic ability of GCLC.^[36,37] Many laboratories have reported a transcriptional induction in one or both of the GCL genes with a wide range of inducers in different cell types.^[38] It is possible that GCL activity is regulated post-translationally. One study reported that treatment of Jurkat cells with ionizing radiation and other model oxidants acutely activated GCL without affecting GCLC or GCLM protein levels. The report proposed a mechanism of post-translational activation whereby an increased proportion of GCL in the holoenzyme form compared to the inactive monomeric form results in high activity and GSH production.^[39] Another interpretation is that the high level of damage switches the redox rheostat towards a pro-oxidant inflammatory response.^[20] This second interpretation would suggest that this enzyme would be an ideal biomarker for assessing damage, and mitigators aimed at increasing its expression would be of value.

Glutathione s-Transferases—(GSTs) are a large family of enzymes that conjugate glutathione to electrophilic centers on a wide variety of substances and are therefore involved in detoxification of xenobiotics. GSTs are highly polymorphic^[40] and different variants exist in different tissues.^[21] Within the GST superfamily, GST π is known to inhibit c-Jun N-terminal kinase (JNK) nonenzymatically to prevent JNK activation and apoptosis.^[41] Radiation-induced oxidative stress can block this interaction to induce apoptosis. GSTM1 can also regulate apoptosis through signal-regulating kinase (ASK1), which activates JNK and p38 pathways.^[42] Interestingly, in our experiment we observed consistent decreases in GST Mu1 levels across strains and genders. The same pattern for GST was also observed in our discovery proteomic experiment from mouse bone marrow using the same irradiation treatment, in which GSTM1 and GSTP1 both progressively decreased over the course of 30 days after irradiation (data not shown). Similar findings for GST radiation response have been reported by other groups. Cholon et al. observed an initial decreased level of GST activity and in cytosolic GST pi isoform in CHO cells after 4.5 Gy of ionizing radiation.^[43] In their study, they only examined π and α isoforms of GST and they classified π isozyme as an early response gene to ionizing radiation. Adams *et al.* also found lower *in vivo* mouse bone marrow GST levels after 2 Gy.^[44] They also discovered that the major changes in GSH and GST occurred in the granulocytes of the bone marrow.^[44] Based on these results, GST protein is radiation responsive and potentially dose-dependent. Furthermore, GST isoforms are tissue-specific, which suggests it to be a desirable biomarker candidate for tissue-specific diagnosis.

Heme oxygenase 1—(HO-1) is an inducible enzyme that catalyzes degradation of heme to biliverdin, CO, and iron. Heme oxygenase is abundant in tissues that degrade aged red blood cells, such as the spleen, liver and bone marrow. When red blood cells are lysed, free heme is released and can cross cell membranes to cause oxidative stress.^[45] By breaking down toxic heme, HO plays a critical role in vascular biology, iron recycling and cellular protection against oxidative stress.^[46] In the context of radiation, HO-1 and CO are found to participate in DNA-repair through the ATM protein.^[47] In our data, HO-1 peaked at Day 1–2 for C57 male mice and Day 2 for C3H male mice (Figure 1). McDonald *et al.* found a dose-dependent increase in HO-1 mRNA expression as well as protein level in mouse

embryonic fibroblast cells irradiated daily with 0.5, 2, or 4 Gy for 5 days.^[18] They further tested *in vivo* response, in which they also observed a significant increase in HO-1 levels in the spleens of C57Bl/6 mice irradiated with 2 Gy whole body every 24 hours for 5 days.^[18] For HO-1, there seems to be good correlation between mRNA expression and protein levels, which suggests the protein level changes are primarily caused by transcriptional activation by ionizing radiation.

Superoxide dismutase (SOD1) and catalase (CAT)—work coordinately to scavenge and detoxify reactive oxygen species and are essential for antioxidant defense in radiation responses. SOD1 converts free radicals to hydrogen peroxide, and CAT then breaks down H₂O₂ to H₂O. As such they are involved in apoptosis and cell death. SOD1 is present in the mitochondria and cytosol of virtually all eukaryotic cells and catalase is mostly located in peroxisomes. For these two enzymes, we observed complex wave-like patterns in response to radiation. Besides catalase, glutathione peroxidases (GPX) also detoxify H₂O₂, and the relative contribution of CAT and GPX to H₂O₂ removal is cell type and tissue dependent.^[48] The relationships between these antioxidants is further complicated by induction of SOD1 through pro-inflammatory pathways that could be involved in our experiments.^[20]

3.5 Gender and strain differences in radiation response

Both strain and gender differences were detected from our protein measurements. It is known that genetic variations in a population contribute to considerable differences in radiation response.^[49–51] Previously, Wright's group observed genotype-dependent responses in bone marrow from C57Bl/6 and CBA/Ca strains after 4 Gy γ -irradiation;^[52] they explained the differences in response as a result of different bone marrow macrophage activities, in which CBA/Ca tissue showed damaging inflammatory-type response, whereas C57Bl/6 bone marrow showed anti-inflammatory or protective response.^[53] Taking this diversity in radiation response into account, a consensus has been established by the radiation medical countermeasure community to test more than one mouse strain in development of radiation protectors and mitigators.^[54] Specifically, C57Bl/6 and C3H/HeN strains are recommended, for which the most data are available and divergence in tissue responses to radiation has been demonstrated.^[54] C57Bl/6 mice are more radioresistant to hematopoietic ARS than C3H mice, which can be explained by more common myeloid progenitor cells in the bone marrow, and in our data they also gave a stronger response of Nrf2-regulated antioxidant proteins to 6 Gy TBI.

A few radiobiology studies have reported gender difference in radiation sensitivity. In our study, within each strain, male mice appeared to have more occurrences of upregulation of these antioxidant enzymes than female mice. The most prominent example is HO-1, in which male mice of both strains showed upregulation in either Day 1 or Day 2 whereas female mice did not (Figure 3). A recent study investigated gender differences in genome damage in prepubertal and adult mice following 8 Gy gamma radiation using an *in vivo* micronucleus assay.^[55] Irradiation caused higher frequency of micronuclei in males of both age groups.^[55] Other studies have also shown that male mice sustained more radiation damage than female mice given the same exposure.^[56,57] Sex hormones, particularly estrogen, have been suggested to play a radioprotective role. Interestingly, a more

fundamental study has looked at the inherent difference in cell death programs between the genders.^[58] The authors proposed that male mice are more prone to PARP-1 necrosis (inflammatory cell death), whereas female mice are more prone to cascade-dependent apoptosis (non-inflammatory cell death) and that estrogen mediates this gender-biased cell death.

The trend of gender difference in radiation sensitivity seems to be translatable from mice to human. Although very few clinical studies on gender-specific differences in radiation sensitivity are available, a number of epidemiological studies have reported such differences in radiation-induced cancer incidence and mortality. In the Life Span Study of atomic bomb survivors, women were found to have a significantly lower risk than men in development of radiation-associated leukemia.^[59] To draw more definitive conclusions about gender differences in radiation response, more systematic radiobiological studies using various cell or animal models of both genders are needed.

4. Concluding remarks

This study reveals time dependent changes in Nrf2-regulated proteins in mouse bone marrow following 6 Gy whole body irradiation in representative mouse strains of both genders. Despite the complexity of the bone marrow tissue environment, we observed some prominent patterns. Among these, the most consistent trend across all mouse models is the decreased abundance of glutathione S-transferase Mu1 isoform. GSTM1 and related isoforms appear to be promising biomarker candidates and their radiation response in blood plasma and dose dependency should be further evaluated. Other patterns, including biphasic responses, are strain or gender-specific.

An ideal radiation injury biomarker should satisfy the following criteria. First, it should be readily obtainable (e.g. serum, urine, saliva, sweat); second, the response should be radiation dose-dependent; third, it should be persistent during the triage timeframe; last, the response should be radiation-specific and not confounded by other stressors. Nrf2-regulated proteins have the potential to fulfill these requirements based on previous experimental evidence of robust and dose-dependent activation following IR and importance of this pathway in radiation response.^[18,19] Beyond the set of Nrf2-regulated proteins measured in this experiment, other Nrf2-induced proteins are worth investigating in future experiments for their biomarker potential, such as the proteins encoding the genes that were potentially induced in the recent transcriptional study by Purbey *et al.*^[19]

Given that bone marrow is the major blood forming organ, this result can be indicative of detectable changes in blood. This study establishes a targeted MS workflow and provides the basis for future development of organ-specific protein biomarkers used in diagnostic blood test for radiation injury. We acknowledge that these potential markers discovered from tissue will be highly diluted once in the blood stream. To target low abundance protein biomarkers in blood, antibody enrichment strategies may be needed, such as affinity capture of either intact proteins from larger volumes of blood or of peptides using peptide-directed antibodies (e.g., Stable Isotope Standards and Capture by Anti-Peptide Antibodies or SISCAPA).^[60] SISCAPA combines the sensitivity of antibody enrichment with the specificity of targeted

MS detection, offering a solution to bridge discovery and validation of biomarkers, which is beyond the scope of the current study.

Biomarkers for radiation injury not only serves diagnostic or predictive purposes for triage, they are also extremely valuable in radiation countermeasure drug development, in which typical human clinical trials for radiation is not possible and biomarkers are needed to reflect mitigation effects and demonstrate efficacy of new drugs.^[3]

Supplementary Material

Refer to Web version on PubMed Central for supplementary material.

Acknowledgements

This work is supported by NIH R01AI101888 and Postgraduate Scholarship-Doctoral from Natural Sciences and Engineering Research Council of Canada (NSERC PGS-D). We would like to thank Amanda Paulovich for insightful feedback and comments. We also thank the support from Skyline and MSstats teams.

List of Abbreviations:

Nrf2	NF-E2-Related Factor 2
IR	ionizing radiation
ROS	reactive oxygen species
ARS	acute radiation syndrome
ARE	Antioxidant Response Element
GST	glutathione S-transferase
UGT	UDP-glucuronosyltransferase
γ-GCS	γ -glutamylcysteine synthetase
GCL	glutamate-cysteine ligase
GP	glutathione peroxidase
SOD	superoxide dismutase
HO or HMOX	heme oxygenase
CAT	catalase
NQO: NADPH	quinone oxidoreductase
TBI	total body irradiation
TEAB	triethylammonium bicarbonate
SIS	stable isotope-labeled standard
GSH	glutathione

JNK	c-Jun N-terminal kinase
ASK	apoptosis signal-regulating kinase
PARP-1	poly [ADP-ribose] polymerase 1
SISCAPA	Stable Isotope Standards and Capture by Anti-Peptide Antibodies
BMDM	bone marrow derived macrophages

REFERENCES

- [1]. Swartz HM, Flood AB, Gougelet RM, Rea ME, Nicolalde RJ, Williams BB, Health Phys. 2010, 98, 95. [PubMed: 20065671]
- [2]. Sproull M, Camphausen K, Radiat. Res 2016, 186, 423. [PubMed: 27710702]
- [3]. Singh VK, Newman VL, Romaine PL, Hauer-Jensen M, Pollard HB, Expert Rev. Mol. Diagn 2016, 16, 65. [PubMed: 26568096]
- [4]. Leszczynski D, Proteomics 2014, 14, 481. [PubMed: 24376023]
- [5]. Lim Y-B, Pyun B-J, Lee H-J, Jeon S-R, Jin YB, Lee Y-S, Proteomics 2011, 11, 1254. [PubMed: 21319302]
- [6]. Azimzadeh O, Atkinson MJ, Tapio S, Radiat. Environ. Biophys 2014, 53, 31. [PubMed: 24105449]
- [7]. Marchetti F, Coleman MA, Jones IM, Wyrobek AJ, Int. J. Radiat. Biol 2006, 82, 605. [PubMed: 17050475]
- [8]. Ossetrova NI, Sandgren DJ, Blakely WF, Radiat. Prot. Dosimetry 2014, 159, 61. [PubMed: 24925901]
- [9]. Kulkarni S, Koller A, Mani KM, Wen R, Alfieri A, Saha S, Wang J, Patel P, Bandeira N, Guha C, Chen EI, Int. J. Radiat. Oncol 2016, 96, 566.
- [10]. Byrum SD, Burdine MS, Orr L, Mackintosh SG, Authier S, Pouliot M, Hauer-Jensen M, Tackett AJ, PLoS One 2017, 12, e0174771.
- [11]. Whiteaker JR, Zhao L, Saul R, Kaczmarczyk JA, Schoenherr RM, Moore HD, Jones-Weinert C, Ivey RG, Lin C, Hiltke T, Reding KW, Whiteley G, Wang P, Paulovich AG, Radiat. Res 2018, 189, 505. [PubMed: 29474155]
- [12]. Spitz DR, Azzam EI, Jian Li J, Gius D, Cancer Metastasis Rev. 2004, 23, 311. [PubMed: 15197331]
- [13]. Spitz DR, Hauer-Jensen M, Antioxid. Redox Signal 2014, 20, 1407. [PubMed: 24354361]
- [14]. Kobayashi M, Yamamoto M, Antioxid. Redox Signal n.d., 7, 385. [PubMed: 15706085]
- [15]. Lee J-M, Li J, Johnson DA, Stein TD, Kraft AD, Calkins MJ, Jakel RJ, Johnson JA, FASEB J. 2005, 19, 1061. [PubMed: 15985529]
- [16]. Kensler TW, Wakabayashi N, Biswal S, Annu. Rev. Pharmacol. Toxicol 2007, 47, 89. [PubMed: 16968214]
- [17]. TSUKIMOTO M, TAMAISHI N, HOMMA T, KOJIMA S, J. Radiat. Res 2010, 51, 349. [PubMed: 20410673]
- [18]. McDonald JT, Kim K, Norris AJ, Vlashi E, Phillips TM, Lagadec C, Della Donna L, Ratikan J, Szelag H, Hlatky L, McBride WH, Cancer Res. 2010, 70, 8886. [PubMed: 20940400]
- [19]. Purbey PK, Scumpia PO, Kim PJ, Tong A-J, Iwamoto KS, McBride WH, Smale ST, Immunity 2017, 47, 421. [PubMed: 28930658]
- [20]. Murray D, Mirzayans R, McBride WH, Radiat. Res 2018, 190, 331. [PubMed: 30040046]
- [21]. Knight TR, Choudhuri S, Klaassen CD, Toxicol. Sci 2007, 100, 513. [PubMed: 17890767]
- [22]. Wright EG, Int. J. Radiat. Biol 2007, 83, 813. [PubMed: 18058369]

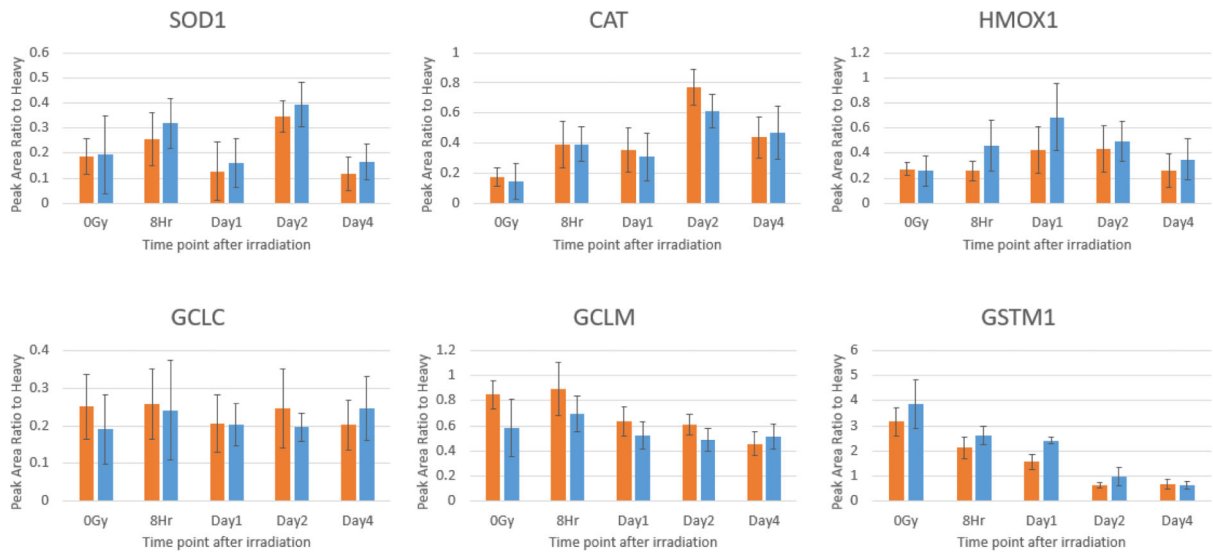
- [23]. Kim J-H, Thimmulappa RK, Kumar V, Cui W, Kumar S, Kombairaju P, Zhang H, Margolick J, Matsui W, Macvittie T, V Malhotra S, Biswal S, J. Clin. Invest 2014, 124, 730. [PubMed: 24463449]
- [24]. Chute JP, J. Clin. Invest 2014, 124, 960. [PubMed: 24569364]
- [25]. Teng P, Bateman NW, Hood BL, Conrads TP, Proteome Res J. 2010, 9, 6091.
- [26]. Mohammed Y, Percy AJ, Chambers AG, Borchers CH, Proteome Res J. 2015, 14, 1137.
- [27]. Percy AJ, Chambers AG, Smith DS, Borchers CH, Proteome Res J. 2013, 12, 222.
- [28]. Percy AJ, Chambers AG, Yang J, Hardie DB, Borchers CH, Biochim. Biophys. Acta - Proteins Proteomics 2014, 1844, 917.
- [29]. Percy AJ, Yang J, Chambers AG, Simon R, Hardie DB, Borchers CH, Proteome Res J. 2014, 13, 3733.
- [30]. Oberg AL, Vitek O, Proteome Res J. 2009, 8, 2144.
- [31]. Choi M, Chang C-Y, Clough T, Broudy D, Killeen T, MacLean B, Vitek O, Bioinformatics 2014, 30, 2524. [PubMed: 24794931]
- [32]. Rodrigues-Moreira S, Moreno SG, Ghinatti G, Lewandowski D, Hoffschir F, Ferri F, Gallouet A-S, Gay D, Motohashi H, Yamamoto M, Joiner MC, Gault N, Romeo P-H, Cell Rep. 2017, 20, 3199. [PubMed: 28954235]
- [33]. Green DE, Rubin CT, Bone 2014, 63, 87. [PubMed: 24607941]
- [34]. Lu SC, Mol. Aspects Med 2009, 30, 42. [PubMed: 18601945]
- [35]. Chan JY, Kwong M, Biochim. Biophys. Acta - Gene Struct. Expr 2000, 1517, 19.
- [36]. Yang Y, Chen Y, Johansson E, Schneider SN, Shertzer HG, Nebert DW, Dalton TP, Biochem. Pharmacol 2007, 74, 372. [PubMed: 17517378]
- [37]. Chen Y, Shertzer HG, Schneider SN, Nebert DW, Dalton TP, J. Biol. Chem 2005, 280, 33766. [PubMed: 16081425]
- [38]. Krzywanski DM, Dickinson DA, Iles KE, Wigley AF, Franklin CC, Liu RM, Kavanagh TJ, Forman HJ, Arch. Biochem. Biophys 2004, 423, 116. [PubMed: 14871475]
- [39]. Krejsa CM, Franklin CC, White CC, Ledbetter JA, Schieven GL, Kavanagh TJ, J. Biol. Chem 2010, 285, 16116. [PubMed: 20332089]
- [40]. Ginsberg G, Smolenski S, Hattis D, Guyton KZ, Johns DO, Sonawane B, J. Toxicol. Environ. Heal. Part B 2009, 12, 389.
- [41]. Wang T, Arifoglu P, Ronai Z, Tew KD, J. Biol. Chem 2001, 276, 20999. [PubMed: 11279197]
- [42]. Cho SG, Lee YH, Park HS, Ryoo K, Kang KW, Park J, Eom SJ, Kim MJ, Chang TS, Choi SY, Shim J, Kim Y, Dong MS, Lee MJ, Kim SG, Ichijo H, Choi EJ, J. Biol. Chem 2001, 276, 12749. [PubMed: 11278289]
- [43]. Cholon A, Giaccia AJ, Lewis AD, Hickson I, Brown JM, Int. J. Radiat. Oncol. Biol. Phys 1992, 22, 759. [PubMed: 1544849]
- [44]. Adams KJ, Carmichael J, Wolf CR, Cancer Res 1985, 45, 1669. [PubMed: 3978635]
- [45]. Fraser ST, Midwinter RG, Berger BS, Stocker R, Adv. Hematol 2011, 2011, 473709.
- [46]. Fraser ST, Midwinter RG, Berger BS, Stocker R, Adv. Hematol 2011, 2011, 473709.
- [47]. Otterbein LE, Hedblom A, Harris C, Csizmadia E, Gallo D, Wegiel B, Proc. Natl. Acad. Sci. U. S. A 2011, 108, 14491. [PubMed: 21849621]
- [48]. Halliwell B, Gutteridge JMC, Free Radicals in Biology and Medicine, Oxford University Press, 2015.
- [49]. Mori N, Okumoto M, Yonezawa M, Nishikawa R, Takamori Y, Esaki K, J. Radiat. Res 1994, 35, 1. [PubMed: 8057265]
- [50]. Kohn HI, Kallman RF, Radiat. Res 1956, 5, 309. [PubMed: 13370831]
- [51]. Roderick TH, Radiat. Res 1963, 20, 631. [PubMed: 14102482]
- [52]. Chen C, Lorimore SA, Evans CA, Whetton AD, Wright EG, Proteomics 2005, 5, 4254. [PubMed: 16196097]
- [53]. Coates PJ, Rundle JK, Lorimore SA, Wright EG, 2008, DOI 10.1158/0008-5472.CAN-07-3050.

- [54]. Williams JP, Brown SL, Georges GE, Hauer-Jensen M, Hill RP, Huser AK, Kirsch DG, Macvittie TJ, Mason KA, Medhora MM, Moulder JE, Okunieff P, Otterson MF, Robbins ME, Smathers JB, McBride WH, *Radiat. Res* 2010, 173, 557. [PubMed: 20334528]
- [55]. Stojkovi R, Fucic A, Ivankovi D, Juki Z, Radulovi P, Grah J, Kova evi N, Bariši L, Krušlin B, *Arch. Ind. Hyg. Toxicol* 2016, 67, 297.
- [56]. Pogribny I, Raiche J, Slovack M, Kovalchuk O, *Biochem. Biophys. Res. Commun* 2004, 320, 1253. [PubMed: 15249225]
- [57]. Ilnytsky Y, Zemp FJ, Koturbash I, Kovalchuk O, *Biochem. Biophys. Res. Commun* 2008, 377, 41. [PubMed: 18823940]
- [58]. Jog NR, Caricchio R, *Cell Death Dis.* 2013, 4, e758. [PubMed: 23928697]
- [59]. Hsu W-L, Preston DL, Soda M, Sugiyama H, Funamoto S, Kodama K, Kimura A, Kamada N, Dohy H, Tomonaga M, Iwanaga M, Miyazaki Y, Cullings HM, Suyama A, Ozasa K, Shore RE, Mabuchi K, *Radiat. Res* 2013, 179, 361. [PubMed: 23398354]
- [60]. Anderson NL, Anderson NG, Haines LR, Hardie DB, Olafson RW, Pearson TW, *Proteome Res J.* 2004, 3, 235.

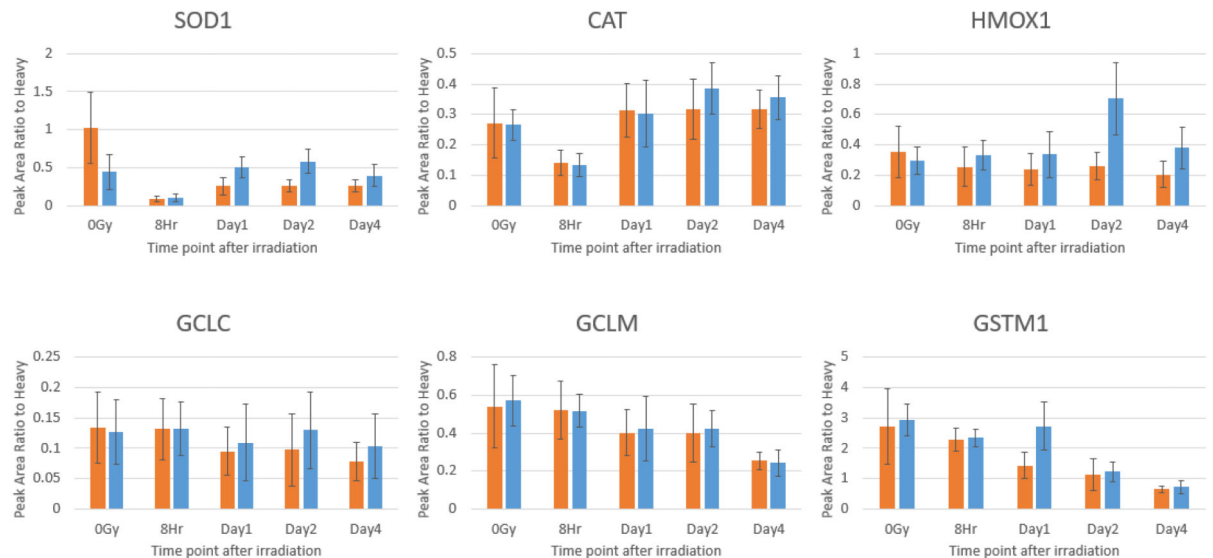
STATEMENT OF CLINICAL RELEVANCE

The threat of radiological and nuclear terrorism has been a concern for national security for years, yet there is still a lack of effective diagnostic procedures for guiding triage and treatment decisions following a radiation incident. Radiation injury can take days, weeks, or even months to present clinical manifestations, which can cause delays in treatment decisions and loss of lives. Moreover, estimate of radiation exposure dose alone is not sufficient because there is considerable individual difference in radiation sensitivity. This leads to the need for radiation injury biomarkers that can confirm exposure and predict acute and delayed radiation injury to different organs and tissues in individual radiation victims. To this end, we performed targeted proteomics experiments on a set of antioxidant response proteins with hypothesized biomarker potential. The Nrf2-mediated response proteins were chosen initially because of previously observed dose-dependent activation of antioxidant response element (ARE)-dependent transcription via Nrf2 after ionizing radiation. Given bone marrow's role in hematopoietic acute radiation syndrome and its function as a blood forming organ, the protein responses measured in bone marrow in this study are likely indicative of changes in blood before subsequent investigations on their presence in blood plasma toward development of diagnostic blood tests.

(a) C57Bl/6 mice



(b) C3H mice

**Figure 1.**

Time-dependent antioxidant enzyme response in mouse bone marrow (n=8) following 6 Gy TBI as represented by relative peak area ratios of endogenous to SIS peptides obtained from Skyline. (a) C57Bl/6 male (blue) and female (orange) mice, (b) C3H male (blue) and female (orange) mice. Error bars indicate standard errors of the mean ratios from both biological and technical replicates.

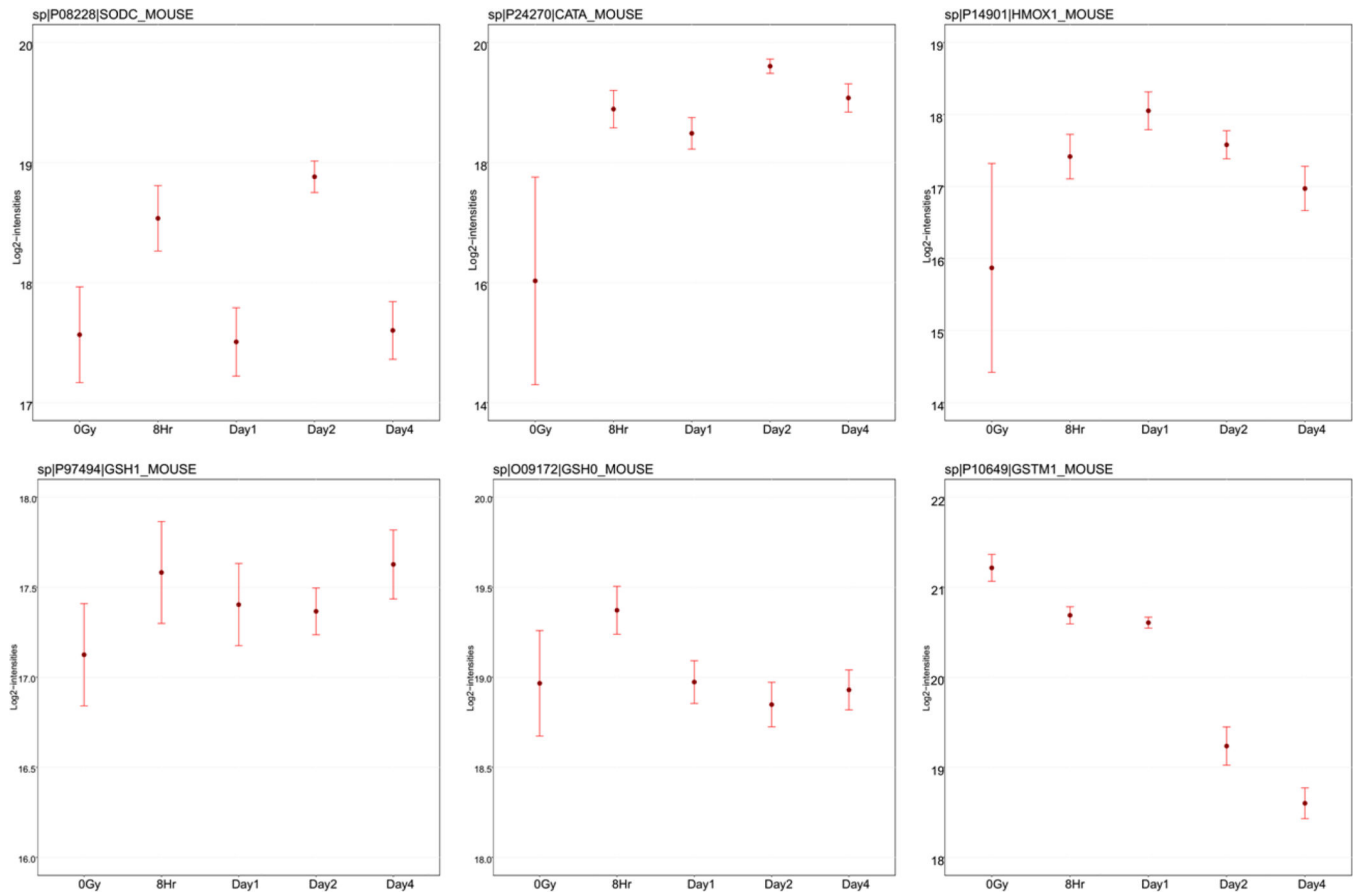


Figure 2.

Condition plots for refined protein intensities in bone marrow of C57Bl/6 male mice after 6 Gy TBI. Dots indicate the mean of log₂ intensities for each time point. Error bars indicate the confidence interval with 0.95 significant level for each time point.

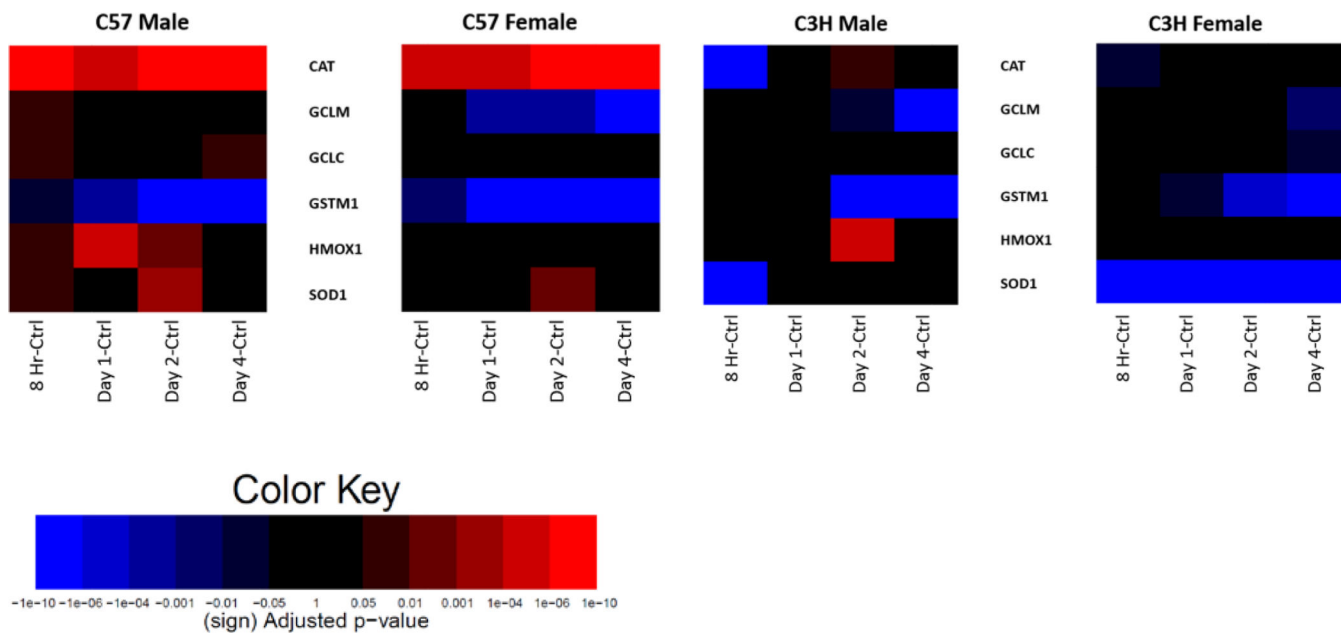


Figure 3. Statistically significance of protein changes in mouse bone marrow at 8 h, Day 1, Day 2, and Day 4 after 6 Gy TBI compared to unirradiated control in each strain/gender group (n=8). Columns in the heatmaps are comparisons of time points relative to control, and rows are proteins. The heatmaps display signed FDR-adjusted p-values using the Benjamini and Hochberg approach. Negative sign (blue) indicates down-regulation; positive sign (red) indicates up-regulation. Brighter color represents stronger differential abundance. Black color represents no significant differential abundance.

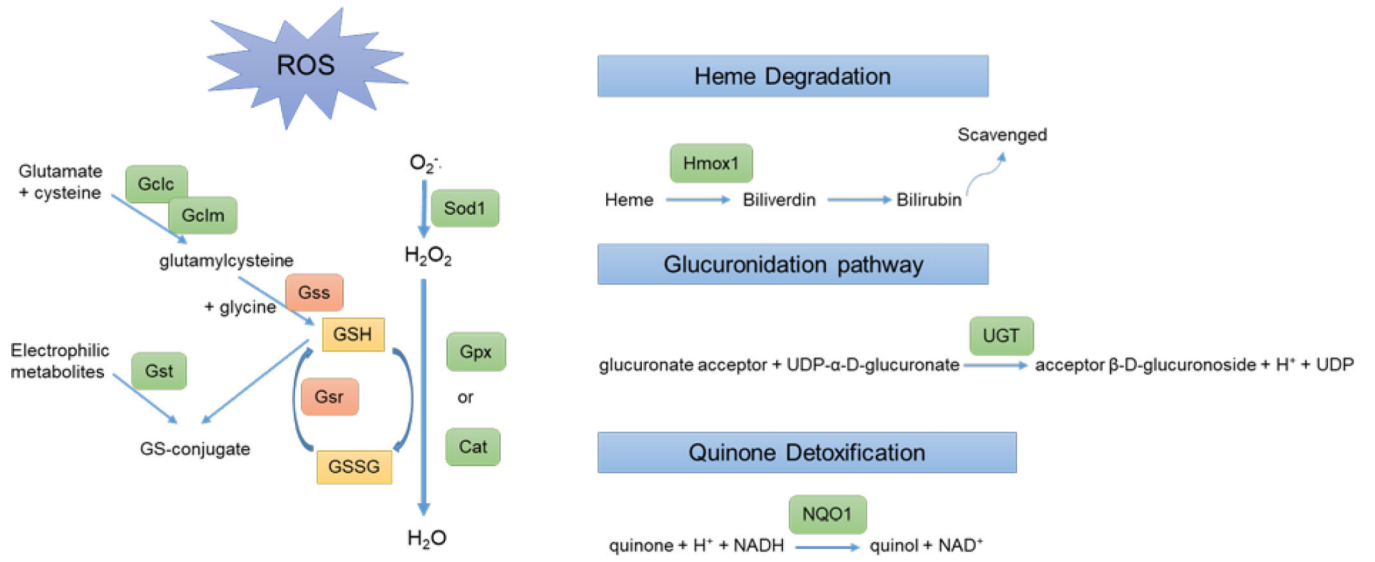


Figure 4. Schematic diagram of Nrf2 regulated antioxidants and xenobiotic pathways. The enzymes measured in this study are indicated by green boxes.

Table 1.

Target proteins and their surrogate peptides.

Protein Name	Gene (Protein Abbrev.)	Peptide	Mass [m/z]
catalase	CAT	FNSANEDNVTQV(R)	747.35
		NFTOVHPDYGA(R)	464.55
glutathione peroxidase 1	GPX1	YVRPGGGFEPNFTLFE(K)	653.33
		AHPLFTFL(R)	367.88
glutamate-cysteine ligase regulatory subunit	GCLM (GSHO)	LFIVGSNSSSST(R)	677.85
		IVAIGTSDLD(K)	566.32
glutamate-cysteine ligase catalytic subunit	GCLC (GSH 1}	SLFFPDEAIN(K)	640.83
		WINVPIF(K)	514.83
glutathione S-transferase Mu1	GSTM1	ITQSNAIL(R) *	508.30
		YIATPIFS(K)	520.29
heme oxygenase 1	HMOXI(HO-1)	THPELLVAHAYT(R)	754.40
		YLGDLGGQVL(K)	625.34
NADPH dehydrogenase [quinone] 1	NADPH1 (NQO1)	NFQYPSESSLAY(K)	767.36
		FGLSVGHHLG(K)	576.32
superoxide dismutase [Cu-Zn]	SOD1	GDGPVQGTIHFEQ(K)	756.88
		HVGDLDGNVTAG(K)	584.31
UDP-glucuronosyltransferase 1-1	UGT 1-1	GHEVWIAPEASIH(K)	566.99
		YTGTRPSNLA(K) *	604.33

* These peptides are not unique to the protein isoform. Bolded peptides are the final 6 surrogate peptides used in quantitation.